AIMS Mathematics, 7(7): 11718–11731.
DOI:10.3934/math.2022653
Received: 24 February 2022
Revised: 28 March 2022
Accepted: 06 April 2022
Published: 18 April 2022

http://www.aimspress.com/journal/Math

Research article

Generalized perimantanes diamondoid structure and their edge-based metric dimensions

Al-Nashri Al-Hossain Ahmad[1] **and Ali Ahmad**[2,*]

[1] Department of Mathematics, AL Qunfudha University College, Umm AL-Qura University, Saudi Arabia

[2] College of Computer Science and Information Technology, Jazan University, Jazan, Saudi Arabia

* **Correspondence:** Email: ahmadsms@gmail.com; Tel: +966595889726.

Abstract: Due to its superlative physical qualities and its beauty, the diamond is a renowned structure. While the green-colored perimantanes diamondoid is one of a higher diamond structure. Motivated by the structure's applications and usage, we look into the edge-based metric parameters of this structure. In this draft, we have discussed edge metric dimension and their generalizations for the generalized perimantanes diamondoid structure and proved that each parameter depends on the copies of original or base perimantanes diamondoid structure and changes with the parameter λ or its number of copies.

Keywords: mixed metric dimension; edge metric dimension; generalized perimantanes diamondoids; diamond structure; edge resolving set
Mathematics Subject Classification: 05C09, 05C12, 05C92

1. Introduction

Due to its superlative physical qualities and its beauty, the diamond is a renowned structure. Polishing, drilling, cutting, and heatsink in electronics are numerous practical and industrial applications of diamond. Its hardness, exceptional thermal conductivity determines by its rigor of composition. A single molecule with macroscopic size makes it into a diamond crystal. The model depicting fundamental atomic groupings undergoes alterations while going from molecules to materials, both in terms of idea and actual manifestation, as well as insignificant computational processing [1].

There are four types of higher diamondoids and each have been assigned with four different colors and name. The assigned colors are yellow, red, blue, and green, while the names are, nonbranched rodlike zigzag catamantanes associated with yellow. The regularly branched catamantanes are linked

with blue diamondoids, chiral diamondoids are red-colored and the green-colored are perimantanes diamondoids. All these series have been isolated and found from petroleum [2].

A chemical/molecular graph is a hydrogen-depleted molecular structure in which the edges represent bonds and the vertices represent atoms in the underlying organic chemical compounds. The chemical graph theory is the study of these chemical graphs [3, 4]. There are enough data available on this assumption and transformation from a chemical structure to a graph (vertex-edge-based structure). More detail can be found in the recent literature such as [5–7].

The notion of resolving set was proposed by the researcher in [8]. It is the first study to look at the notion of finding a graph's metric dimension using the definition of a resolving set. The least cardinality of a resolving set is the metric dimension. The impetus for inventing the notion of finding the set came from LORAN and sonar stations. After that, several academics took this concept and labeled it in a variety of ways. The idea of a resolving set is dubbed as a metric dimension in [9]'s study. While the researchers in [10, 11] renamed the same notion with metric foundation or resolving set in a purely theoretical fashion. A more advanced definition of a resolving set was developed in the last decade. Researchers of [12] in which the idea of edge resolving set is explained. The notion is referred to as a fault-tolerant edge resolving set is defined in [13], and it is a generalized form of the edge resolving set. A Further generalized version of edge and resolving set is named as mixed-metric resolving set is defined in [14].

Many concepts and implementations sprang from the generalized approach of resolving set. In electronics [15], a recent innovation reveals the implementation of locating set (and its extensions). A method for studying diverse polyphenyl structures, especially for the polymer industry citation Nadeem2021b. In the broader view, this idea is used in combinatorial optimization [16], some complex games or robotic roving [17], image processing [8], pharmaceutical chemistry [18].

The job of determining a graph's resolving set is a non-deterministic polynomial-time hard problem (NP), with an unknown algorithmic difficulty [19–21]. Metric dimension or resolving set has a large literature because of its many variations and applications in various disciplines. Few research are discussed by [22–29]. There is extensive research on the edge metric only the most current and broad results will be discussed here. A generalized structure of convex polytopes are discussed in [30], barycentric is an operation of graph discussed in [31], study of edge and its base parameter studied in [32], necklace structure is discussed in [33], generalized version of edge resolving set is discussed in [34, 35], computer networks and their edge metric based parameters are studied in [36–38]. For the mixed metric, [39] studied the generalized Peterson graph, rotational symmetric graph is discussed in [40], generalized path related graphs are studied in [41], generalized class of an aromatic compound are studied in [42, 43], quartz based structure discussed in [44]. Moreover, some recent studies and literature are available at [45, 46].

Given below are some basic concepts elaborated for further use in our main results.

Definition 1.1. [12, 37] *A vertex $\alpha \in V(G)$ and a branch $e = \alpha_1\alpha_2 \in E(G)$, the distance between α and edge e is defined as $d(e, \alpha) = min\{d(\alpha_1, \alpha), d(\alpha_2, \alpha)\}$. Suppose $R_e \subset V(G)$ is the subset of vertex set and defined as $R_e = \{\alpha_1, \alpha_2, \ldots, \alpha_s\}$, and a branch $e \in E(\alpha)$. The identification $r(e|R_e)$ of a branch e with respect to R_e is actually a $s-$tuple distances $(d(e, \alpha_1), d(e, \alpha_2), \ldots, d(e, \alpha_s))$. If each branch from $E(G)$ have unique identification according to R_e, then R_e is called an edge metric resolving set of network $\aleph$. The minimum count of the elements in R_e is called the edge metric dimension of $\aleph$ and it is represented by $dim_e(G)$.*

Definition 1.2. [13,37] *An edge metric resolving set R_e of a network G is said to be fault-tolerant edge metric ($R_{e,f}$) if for each $\alpha \in R_e$, $R_e \backslash \alpha$ is also a edge metric resolving set for G. The minimum amount of the fault-tolerant edge metric resolving set is known as the fault-tolerant edge metric dimension and described as $dim_{e,f}(\alpha)$.*

Definition 1.3. [36] *A vertex α of a connected associated graph G of a chemical structure, differentiates nodes (α_1) and edges (e_1), if $d(\alpha_1, \alpha) \neq d(\alpha, e_1)$. A subset R_m is a mixed resolving set if any different pair of components of G are separated by a node of R_m. The minimum number of nodes in mixed resolving set for G is named the mixed metric dimension and is denoted by $dim_m(G)$. It is also known as blended version of both metric* [8] *and edge metric dimension* [10].

In this draft, we have discussed edge metric dimension and their generalizations for the generalized perimantanes diamondoid structure and proved that each parameter depends on the copies of original or base perimantanes diamondoid structure and changes with the parameter n or its number of copies. The next section will present some main results, conclusions are drawn and at the end, references are given for more and deep insight into this topic and structure.

2. Construction and methodology of presented work

The structure shown in Figure 1, is a green-colored perimantanes diamondoid and one of a higher diamond structure. Its topological version is found in [1,2] and motivated by the structures applications and usage, we look into the metric-based parameters of this structure.

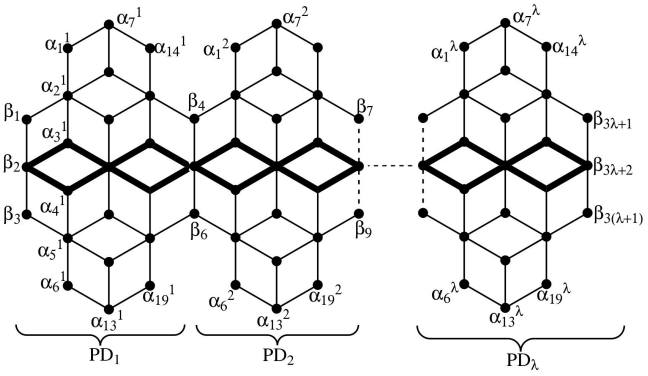

Figure 1. Vertex-edge sets of perimantanes diamondoid structure D_n.

The perimantanes diamondoid structure has total $|V(PD_\lambda)| = 22\lambda + 3$, number of vertices and total edges are $|E(PD_\lambda)| = 38\lambda + 2$. The labeling of vertices and edges is described in Figure 1 and is utilized in the major results. Furthermore, vertex and edge are stated given below.

$$V(PD_\lambda) = \{\alpha_\xi^j : \xi = 1, 2, \ldots, 19,\ j = 1, 2, \ldots, \lambda\} \cup \{\beta_\xi : \xi = 1, 2, \ldots, 3(\lambda + 1)\},$$

$$E(PD_\lambda) = \{\alpha_\xi^j \alpha_{\xi+1}^j : \xi = 1, 2, 4, 5, 7, 9, 10, 12, 14, 15, 17, 18\ j = 1, 2, \ldots, \lambda\} \cup \{\beta_\xi \beta_{\xi+1} : \xi = 1, 4, 7, \ldots, 3\lambda + 1,\ \xi = 2, 5, \ldots, 3\lambda + 1\} \cup \{\beta_\xi \alpha_2^j : \xi = 1, 4, 7, \ldots, 3\lambda - 2,\ j = 1, 2, \ldots, \lambda\} \cup \{\beta_\xi \alpha_3^j,\ \beta_\xi \alpha_4^j : \xi = 2, 5, 8, \ldots, 3\lambda - 1,\ j = 1, 2, \ldots, \lambda\} \cup \{\beta_\xi \alpha_5^j : \xi = 3, 6, 9, \ldots, 3\lambda,\ j = 1, 2, \ldots, \lambda\} \cup \{\beta_\xi \alpha_{15}^j : \xi = 4, 7, 10, \ldots, 3\lambda + 1,\ j = 1, 2, \ldots, \lambda\} \cup \{\beta_\xi \alpha_{16}^j,$$

$\beta_\xi\alpha_{17}^j : \ \xi = 5, 8, 11, \ldots, 3\lambda + 2, \ j = 1, 2, \ldots, \lambda\} \cup \{\beta_\xi\alpha_{18}^j : \ \xi = 6, 9, 12, \ldots, 3\lambda + 3,$
$j = 1, 2, \ldots, \lambda\}.$

Presented below are the main results of this novel structure.

Lemma 2.1. *Let PD_λ is a structure of perimantanes diamondoid with $\lambda \geq 1$, and R_e is the edge resolving set of PD_λ for $\lambda = 1$. Then one of the possible edge resolving set is defined as*

$$R_e = \{\beta_1, \beta_4, \alpha_7^1\}.$$

Proof. Using the definition of edge resolving set and find the locations of each edge with regards to the chosen edge resolving set. Let $R_e = \{\beta_1, \beta_4, \alpha_7^1\}$, is one of a candidate subset and given below are the representations of every edge of structure of perimantanes diamondoid PD_1, and the structure shown in the Figure 1.

$$r\left(\alpha_\xi^j\alpha_{\xi+1}^j|R_e\right) = \begin{cases} (\xi, \xi+2, \xi), & \text{if } \xi = 1; \\ (\xi-1, \xi+1, \xi), & \text{if } \xi = 2; \\ (\xi-2, \xi, \xi+1), & \text{if } \xi = 4; \\ (\xi-5, \xi-5, \xi-7), & \text{if } \xi = 7; \\ (\xi-7, \xi-7, \xi-6), & \text{if } \xi = 9, 10; \\ (\xi-8, \xi-8, \xi-5), & \text{if } \xi = 12; \\ (\xi-11, \xi-13, \xi-13), & \text{if } \xi = 14; \\ (\xi-12, \xi-14, \xi-13), & \text{if } \xi = 15; \\ (\xi-13, \xi-15, \xi-12), & \text{if } \xi = 17; \\ (\xi-13, \xi-15, \xi-12), & \text{if } \xi = 18. \end{cases} \tag{2.1}$$

$$r\left(\beta_\xi\beta_{\xi+1}|R_e\right) = \begin{cases} (\xi-1, 3+\xi, \xi+2), & \text{if } \xi = 1, 2; \\ (\xi, \xi-4, \xi-1), & \text{if } \xi = 4, 5. \end{cases} \tag{2.2}$$

$r\left(\beta_\xi\alpha_2^j|R_e\right) = (0,3,2), r\left(\beta_\xi\alpha_3^j|R_e\right) = (1,4,3), r\left(\beta_\xi\alpha_4^j|R_e\right) = (1,4,4), r\left(\beta_\xi\alpha_5^j|R_e\right) = (2,5,6).$
$r\left(\beta_\xi\alpha_{15}^j|R_e\right) = (3,0,2), r\left(\beta_\xi\alpha_{16}^j|R_e\right) = (4,1,3), r\left(\beta_\xi\alpha_{17}^j|R_e\right) = (4,1,4), r\left(\beta_\xi\alpha_{18}^j|R_e\right) = (5,2,5).$

$$r\left(\alpha_1^j\alpha_7^j|R_e\right) = (2,3,0), \ r\left(\alpha_2^j\alpha_8^j|R_e\right) = (1,2,1), \ r\left(\alpha_2^j\alpha_9^j|R_e\right) = (1,2,2),$$
$$r\left(\alpha_3^j\alpha_{10}^j|R_e\right) = (2,3,3), \ r\left(\alpha_4^j\alpha_{10}^j|R_e\right) = (2,3,4), \ r\left(\alpha_5^j\alpha_{11}^j|R_e\right) = (3,2,6),$$
$$r\left(\alpha_5^j\alpha_{12}^j|R_e\right) = (3,4,6), \ r\left(\alpha_6^j\alpha_{13}^j|R_e\right) = (4,5,7), \ r\left(\alpha_7^j\alpha_{14}^j|R_e\right) = (3,2,0),$$
$$r\left(\alpha_8^j\alpha_{15}^j|R_e\right) = (2,1,1), \ r\left(\alpha_9^j\alpha_{15}^j|R_e\right) = (2,2,2), \ r\left(\alpha_{10}^j\alpha_{16}^j|R_e\right) = (3,2,4),$$
$$r\left(\alpha_{10}^j\alpha_{17}^j|R_e\right) = (3,3,4), \ r\left(\alpha_{11}^j\alpha_{18}^j|R_e\right) = (4,3,5), \ r\left(\alpha_{12}^j\alpha_{18}^j|R_e\right) = (4,3,6),$$
$$r\left(\alpha_{13}^j\alpha_{19}^j|R_e\right) = (5,4,7).$$

It is obvious by looking at the position of every edge, that there are no two edges having the same code. In the short entire structure of perimantanes diamondoid with $\lambda = 1$, has unique representations with regard to the chosen subsets. It is proved that the chosen subset is one of the possible candidates for the edge resolving set with three minimum elements in it. □

Lemma 2.2. *Let PD_λ is a structure of perimantanes diamondoid with $\lambda = 1$. Then*

$$dim_e\,(PD_1) = 3. \tag{2.3}$$

Proof. The subset chosen in the Lemma 2.1 is a base case of this lemma. In the lemma, it is proved that $R_e = \{\beta_1, \beta_4, \alpha_7^1\}$, is one of a candidate subset for the edge resolving set of structure of perimantanes diamondoid PD_1, and the structure shown in the Figure 1. Having three members in it, this proved that $dim_e\,(PD_1) \leq 3$. For the twofold inequality, chose contrary method and we will proved that $dim_e\,(PD_1) \neq 2$. Given below are some reasons on this assertion.

Case 2.1. *Let a chosen subset R'_e having two distinct elements, say $R'_e = \{\beta_1, \beta_2\}$. The contradiction will be arise due the edges which have two distance to any of the chosen element of R'_e. Mathematically, it can be written as $r\left(\alpha_\xi^1|R'_e\right) = r\left(\alpha_j^1|R'_e\right) = d\left(\alpha_\xi^1, \beta_1\right) = 2$.*

Case 2.2. *Let a chosen subset B' having two distinct elements, say $R'_e = \{\beta_1, \beta_3\}$. The contradiction will be arise due the edges which have two distance to any of the chosen element of R'_e. Mathematically, it can be written as $r\left(\alpha_\xi^1|R'_e\right) = r\left(\alpha_j^1|R'_e\right) = d\left(\alpha_\xi^1, \beta_1\right) = 2$.*

Case 2.3. *Let a chosen subset R'_e having two distinct elements, say $R'_e = \{\beta_2, \beta_3\}$. The contradiction will be arise due the edges which have two distance to any of the chosen element of R'_e. Mathematically, it can be written as $r\left(\alpha_\xi^1|R'_e\right) = r\left(\alpha_j^1|R'_e\right) = d\left(\alpha_\xi^1, \beta_1\right) = 2$.*

Case 2.4. *Let a chosen subset R'_e having two distinct elements, say $R'_e = \{\alpha_\xi^1, \alpha_1^j\}$, with distinct ξ, j. The contradiction will be arise due the edges which have two and three distance to any of the chosen element of R'_e. Mathematically, it can be written as $r\left(\alpha_\alpha^1|R'_e\right) = r\left(\alpha_\beta^1|R'_e\right) = d\left(\alpha_\alpha^1, \alpha_\xi^1\right) = \{2, 3\}$.*

All the chosen cases resulted in the same location of at least two edges of the structure and our main assertion resulted in the contradiction. So, it is proved that $dim_e\,(PD_1) \neq 2$.

Hence, $dim_e\,(PD_1) = 3$. □

Theorem 2.1. *Let PD_λ is a structure of perimantanes diamondoid with $\lambda \geq 2$. Then*

$$dim_e\,(PD_\lambda) = \lambda + 2 \tag{2.4}$$

Proof. We will proved that the entire structure of perimantanes diamondoid have $dim_e\,(PD_\lambda) = \lambda+2$ for every possible value of $\lambda \geq 2$. For this prove, we will employ the technique of mathematical induction and the base case, which is for $\lambda = 1$ and $dim_e\,(PD_1) = 3$, is already proved in the Lemmas 2.1 and 2.2. Now, suppose the assertion is true for $\lambda = \chi$, and the equation becomes

$$dim_e\left(PD_\chi\right) = \chi + 2. \tag{2.5}$$

We will show that it is true for $\lambda = \chi + 1$. Suppose

$$dim_e\left(PD_{\chi+1}\right) = dim_e\left(PD_\chi\right) + dim_e\,(PD_1) - 2. \tag{2.6}$$

Using Eqs 2.3 and 2.5 in Eq 2.6, we have

$$\begin{aligned} dim_e\left(PD_{\chi+1}\right) =& \chi + 2 + 3 - 2, \\ =& \chi + 3. \end{aligned} \tag{2.7}$$

As a result, the conclusion holds for all positive integers $\lambda \geq 1$.

Moreover, the generalized edge resolving set for the generalized structure of perimantanes diamondoid, is in the set form is given by $R_e = \{\beta_1, \beta_{3\lambda+1}, \alpha_7^1, \alpha_7^2, \alpha_7^3, \ldots, \alpha_7^\lambda\}$. This concludes. □

Lemma 2.3. *Let PD_λ is a structure of perimantanes diamondoid with $\lambda \geq 1$, and $R_{e,f}$ is the fault-tolerant edge resolving set of PD_λ for $\lambda = 1$. Then one of the possible fault-tolerant edge resolving set is defined as*

$$R_{e,f} = \{\beta_1, \beta_4, \alpha_7^1, \beta_3, \beta_6, \alpha_{13}^1\}.$$

Proof. Using the definition of fault-tolerant edge resolving set and found the locations of each edge with regards to the chosen fault-tolerant edge resolving set. Let $R_{e,f} = \{\beta_1, \beta_4, \alpha_7^1, \beta_3, \beta_6, \alpha_{13}^1\}$, is one of a candidate subset and given below are the representations of every edge of structure of perimantanes diamondoid PD_1, and the structure shown in the Figure 1.

$$r\left(\alpha_\xi^j \alpha_{\xi+1}^j | R_{e,f}\right) = \begin{cases} (\xi, \xi+2, \xi, \xi+2, \xi+4, \xi+5), & \text{if } \xi = 1; \\ (\xi-1, \xi+1, \xi, \xi, \xi+2, \xi+3), & \text{if } \xi = 2; \\ (\xi-2, \xi, \xi+1, \xi-3, \xi-1, \xi-2), & \text{if } \xi = 4; \\ (\xi-5, \xi-5, \xi-7, \xi-3, \xi-3, \xi), & \text{if } \xi = 7; \\ (\xi-7, \xi-7, \xi-6, \xi-6, \xi-6, \xi-5), & \text{if } \xi = 9; \\ (\xi-7, \xi-7, \xi-6, \xi-8, \xi-8, \xi-7), & \text{if } \xi = 10; \\ (\xi-8, \xi-8, \xi-5, \xi-10, \xi-10, \xi-12), & \text{if } \xi = 12; \\ (\xi-11, \xi-13, \xi-13, \xi-9, \xi-11, \xi-8), & \text{if } \xi = 14; \\ (\xi-12, \xi-14, \xi-13, \xi-11, \xi-13, \xi-10), & \text{if } \xi = 15; \\ (\xi-13, \xi-15, \xi-12, \xi-14, \xi-16, \xi-15), & \text{if } \xi = 17; \\ (\xi-13, \xi-15, \xi-12, \xi-15, \xi-17, \xi-17), & \text{if } \xi = 18. \end{cases} \tag{2.8}$$

$$r\left(\beta_\xi \beta_{\xi+1} | R_{e,f}\right) = \begin{cases} (\xi-1, 3+\xi, \xi+2, \xi, \xi+4, \xi+3), & \text{if } \xi = 1; \\ (\xi-1, 3+\xi, \xi+2, \xi-2, \xi+2, \xi+1), & \text{if } \xi = 2; \\ (\xi, \xi-4, \xi-1, \xi+1, \xi-3, \xi), & \text{if } \xi = 4, \\ (\xi, \xi-4, \xi-1, \xi-4, \xi-5, \xi-2), & \text{if } \xi = 5. \end{cases} \tag{2.9}$$

$$\begin{aligned} r\left(\beta_\xi \alpha_2^j | R_{e,f}\right) &= (0, 3, 2, 2, 5, 5), \\ r\left(\beta_\xi \alpha_3^j | R_{e,f}\right) &= (1, 4, 3, 1, 4, 4), \\ r\left(\beta_\xi \alpha_4^j | R_{e,f}\right) &= (1, 4, 4, 1, 4, 3), \\ r\left(\beta_\xi \alpha_5^j | R_{e,f}\right) &= (2, 5, 6, 0, 3, 2). \\ r\left(\beta_\xi \alpha_{15}^j | R_{e,f}\right) &= (3, 0, 2, 5, 2, 5), \\ r\left(\beta_\xi \alpha_{16}^j | R_{e,f}\right) &= (4, 1, 3, 4, 1, 4), \\ r\left(\beta_\xi \alpha_{17}^j | R_{e,f}\right) &= (4, 1, 4, 4, 1, 3), \end{aligned}$$

$$r\left(\beta_{\xi}\alpha_{18}^{j}|R_{e,f}\right) = (5,2,5,3,0,2)\,.$$

$$r\left(\alpha_{1}^{j}\alpha_{7}^{j}|R_{e,f}\right) = (2,3,0,4,5,7)\,,\ r\left(\alpha_{2}^{j}\alpha_{8}^{j}|R_{e,f}\right) = (1,2,1,3,5,6)\,,\ r\left(\alpha_{2}^{j}\alpha_{9}^{j}|R_{e,f}\right) = (1,2,2,3,4,5)\,,$$
$$r\left(\alpha_{3}^{j}\alpha_{10}^{j}|R_{e,f}\right) = (2,3,3,2,3,4)\,,\ r\left(\alpha_{4}^{j}\alpha_{10}^{j}|R_{e,f}\right) = (2,3,4,2,3,3)\,,\ r\left(\alpha_{5}^{j}\alpha_{11}^{j}|R_{e,f}\right) = (3,2,6,1,2,2)\,,$$
$$r\left(\alpha_{5}^{j}\alpha_{12}^{j}|R_{e,f}\right) = (3,4,6,1,2,1)\,,\ r\left(\alpha_{6}^{j}\alpha_{13}^{j}|R_{e,f}\right) = (4,5,7,2,3,0)\,,\ r\left(\alpha_{7}^{j}\alpha_{14}^{j}|R_{e,f}\right) = (3,2,0,5,4,7)\,,$$
$$r\left(\alpha_{8}^{j}\alpha_{15}^{j}|R_{e,f}\right) = (2,1,1,4,3,6)\,,\ r\left(\alpha_{9}^{j}\alpha_{15}^{j}|R_{e,f}\right) = (2,2,2,4,3,5)\,,\ r\left(\alpha_{10}^{j}\alpha_{16}^{j}|R_{e,f}\right) = (3,2,4,3,3,4)\,,$$
$$r\left(\alpha_{10}^{j}\alpha_{17}^{j}|R_{e,f}\right) = (3,3,4,3,2,4)\,,\ r\left(\alpha_{11}^{j}\alpha_{18}^{j}|R_{e,f}\right) = (4,3,5,2,1,2)\,,\ r\left(\alpha_{12}^{j}\alpha_{18}^{j}|R_{e,f}\right) = (4,3,6,2,1,1)\,,$$
$$r\left(\alpha_{13}^{j}\alpha_{19}^{j}|R_{e,f}\right) = (5,4,7,3,2,0)\,.$$

It is obvious by looking at the position of every edge, that there are no two edges having the same code. BY eliminating any element from $R_{e,f}$ making its cardinality five still remains the candidate for the edge resolving set and overall candidate for the fault-tolerant edge resolving set. In short entire structure of perimantanes diamondoid with $\lambda = 1$, have unique representations with regard to the chosen subsets. It is proved that the chosen subset is one of a possible candidate for the fault-tolerant edge resolving set with six minimum elements in it. □

Lemma 2.4. *Let PD_{λ} is a structure of perimantanes diamondoid with $\lambda = 1$. Then*

$$dim_{e,f}\,(PD_1) = 6. \tag{2.10}$$

Proof. The subset chosen in the Lemma 2.3 is a base case of this lemma. In the lemma, it is proved that $R_{e,f} = \{\beta_1, \beta_4, \alpha_7^1, \beta_3, \beta_6, \alpha_{13}^1\}$, is one of a candidate subset for the fault-tolerant edge resolving set of structure of perimantanes diamondoid PD_1, and the structure shown in the Figure 1. Having six members in it, this proved that $dim_{e,f}\,(PD_1) \leq 6$. For the twofold inequality, chose contrary method and we will proved that $dim_{e,f}\,(PD_1) \neq 5$. Given below are some reasons on this assertion.

Let a chosen subset $R'_{e,f}$ having five distinct elements, say $R'_{e,f} = \{\alpha_{\xi}^1, \alpha_1^j\}$, with distinct ξ, j. The contradiction will be arise due the edges which have two and three distance to any of the chosen element of $R'_{e,f}$. Mathematically, it can be written as $r\left(\alpha_{\alpha}^1|R'_{e,f}\right) = r\left(\alpha_{\beta}^1|R'_{e,f}\right) = d\left(\alpha_{\alpha}^1, \alpha_{\xi}^1\right) = \{2,3\}$.

All the chosen cases resulted in the same location of at least two edges of the structure and our main assertion resulted in the contradiction. Either the same locations of edges or by eliminating any vertex from the chosen subset not fulfilling the definition. So, it is proved that $dim_{e,f}\,(PD_1) \neq 5$.
Hence, $dim_{e,f}\,(PD_1) = 6$. □

Theorem 2.2. *Let PD_{λ} is a structure of perimantanes diamondoid with $\lambda \geq 2$. Then*

$$dim_{e,f}\,(PD_{\lambda}) = 2\,(\lambda + 2) \tag{2.11}$$

Proof. We will proved that the entire structure of perimantanes diamondoid have $dim_{e,f}\,(PD_{\lambda})$=$2\,(\lambda + 2)$ for every possible value of $\lambda \geq 2$. For this prove, we will employ the technique of mathematical induction and the base case, which is for $\lambda = 1$ and $dim_{e,f}\,(PD_{\lambda}) = 6$, is already proved in the Lemmas 2.3 and 2.4.

Now, suppose the assertion is true for $\lambda = \chi$, and the equation becomes

$$dim_{e,f}\left(PD_{\chi}\right) = 2\,(\chi + 2)\,. \tag{2.12}$$

We will show that it is true for $\lambda = \chi + 1$. Suppose

$$dim_{e,f}\left(PD_{\chi+1}\right) = dim_{e,f}\left(PD_{\chi}\right) + dim_{e,f}\left(PD_1\right) - 5. \tag{2.13}$$

Using Eqs 2.10 and 2.12 in Eq 2.13, we have

$$\begin{aligned} dim_{e,f}\left(PD_{\chi+1}\right) =& 2\left(\chi + 2\right) + 6 - 5, \\ =& 2\left(\chi + 2\right) + 1. \end{aligned} \tag{2.14}$$

As a result, the conclusion holds for all positive integers $\lambda \geq 1$.

Moreover, the generalized fault-tolerant edge resolving set for the generalized structure of perimantanes diamondoid, is in the set form is given by $R_{e,f} = \{\beta_1, \beta_3, \beta_{3\lambda+1}, \beta_{3\lambda+3}, \alpha_7^1, \alpha_7^2, \alpha_7^3, \ldots, \alpha_7^\lambda, \alpha_{13}^1, \alpha_{13}^2, \alpha_{13}^3, \ldots, \alpha_{13}^\lambda\}$. This concludes. □

Lemma 2.5. *Let PD_λ is a structure of perimantanes diamondoid with $\lambda \geq 1$, and R_m is the vertex-edge resolving set of PD_λ for $\lambda = 1$. Then one of the possible vertex-edge resolving set is defined as*

$$R_m = \{\beta_1, \beta_4, \alpha_7^1, \alpha_{13}^1\}.$$

Proof. Using the definition of mixed-metric resolving set and found the locations of each edge and vertex with regards to the chosen mixed-metric resolving set. Let $R_m = \{\beta_1, \beta_4, \alpha_7^1, \alpha_{13}^1\}$, is one of a candidate subset and given below are the representations of every edge and vertex of structure of perimantanes diamondoid PD_1, and the structure shown in the Figure 1.

Given below are representations of every vertex of structure of perimantanes diamondoid PD_1, by using the definition of shortest distances. If we found every vertex having unique positions then we will further compute the locations of edges of this structure.

$$r\left(\alpha_\xi^j | R_m\right) = \begin{cases} (3-\xi, 5-\xi, \xi, 8-\xi), & \text{if } \xi = 1, 2; \\ (2, 4, \xi, 8-\xi), & \text{if } \xi = 3; \\ (2, \xi, \xi+1, 7-\xi), & \text{if } \xi = 4; \\ (\xi-2, \xi, \xi+1, 7-\xi), & \text{if } \xi = 5, 6; \\ (10-\xi, 10-\xi, \xi-7, 15-\xi), & \text{if } \xi = 7, 8; \\ (\xi-7, \xi-7, \xi-7, 14-\xi), & \text{if } \xi = 9, 10, 11; \\ (\xi-8, \xi-8, \xi-5, 13-\xi), & \text{if } \xi = 12, 13; \\ (18-\xi, 16-\xi, \xi-13, 20-\xi), & \text{if } \xi = 14, 15; \\ (4, 2, 18-\xi, 20-\xi), & \text{if } \xi = 16; \\ (\xi-13, \xi-15, \xi-12, 20-\xi), & \text{if } \xi = 17, 18, 19. \end{cases} \tag{2.15}$$

$$r\left(\beta_\xi | R_m\right) = \begin{cases} (\xi-1, 3+\xi, \xi+2, 6-\xi), & \text{if } \xi = 1, 2, 3; \\ (\xi, \xi-4, \xi-1, 9-\xi), & \text{if } \xi = 4, 5, 6. \end{cases} \tag{2.16}$$

Given below are representations of every edge of structure of perimantanes diamondoid PD_1, by using the definition of shortest distances. If we found every edge having also unique positions then we will further compare the locations of vertices with edges of this structure.

$$r\left(\alpha_{\xi}^{j}\alpha_{\xi+1}^{j}|R_m\right)=\begin{cases}(\xi,\xi+2,\xi,\xi+5), & \text{if } \xi=1;\\ (\xi-1,\xi+1,\xi,\xi+3), & \text{if } \xi=2;\\ (\xi-2,\xi,\xi+1,\xi-2), & \text{if } \xi=4;\\ (\xi-5,\xi-5,\xi-7,\xi), & \text{if } \xi=7;\\ (\xi-7,\xi-7,\xi-6,\xi-5), & \text{if } \xi=9;\\ (\xi-7,\xi-7,\xi-6,\xi-7), & \text{if } \xi=10;\\ (\xi-8,\xi-8,\xi-5,\xi-12), & \text{if } \xi=12;\\ (\xi-11,\xi-13,\xi-13,\xi-8), & \text{if } \xi=14;\\ (\xi-12,\xi-14,\xi-13,\xi-10), & \text{if } \xi=15;\\ (\xi-13,\xi-15,\xi-12,\xi-15), & \text{if } \xi=17;\\ (\xi-13,\xi-15,\xi-12,\xi-17), & \text{if } \xi=18.\end{cases} \tag{2.17}$$

$$r\left(\beta_{\xi}\beta_{\xi+1}|R_m\right)=\begin{cases}(\xi-1,3+\xi,\xi+2,\xi+3), & \text{if } \xi=1;\\ (\xi-1,3+\xi,\xi+2,\xi+1), & \text{if } \xi=2;\\ (\xi,\xi-4,\xi-1,\xi), & \text{if } \xi=4,\\ (\xi,\xi-4,\xi-1,\xi-2), & \text{if } \xi=5.\end{cases} \tag{2.18}$$

$$\begin{aligned}r\left(\beta_{\xi}\alpha_{2}^{j}|R_m\right)&=(0,3,2,5),\\ r\left(\beta_{\xi}\alpha_{3}^{j}|R_m\right)&=(1,4,3,4),\\ r\left(\beta_{\xi}\alpha_{4}^{j}|R_m\right)&=(1,4,4,3),\\ r\left(\beta_{\xi}\alpha_{5}^{j}|R_m\right)&=(2,5,6,2).\\ r\left(\beta_{\xi}\alpha_{15}^{j}|R_m\right)&=(3,0,2,5),\\ r\left(\beta_{\xi}\alpha_{16}^{j}|R_m\right)&=(4,1,3,4),\\ r\left(\beta_{\xi}\alpha_{17}^{j}|R_m\right)&=(4,1,4,3),\\ r\left(\beta_{\xi}\alpha_{18}^{j}|R_m\right)&=(5,2,5,2).\end{aligned}$$

$$\begin{aligned}r\left(\alpha_{1}^{j}\alpha_{7}^{j}|R_m\right)=(2,3,0,7),\ r\left(\alpha_{2}^{j}\alpha_{8}^{j}|R_m\right)=(1,2,1,6),\ r\left(\alpha_{2}^{j}\alpha_{9}^{j}|R_m\right)=(1,2,2,5),\\ r\left(\alpha_{3}^{j}\alpha_{10}^{j}|R_m\right)=(2,3,3,4),\ r\left(\alpha_{4}^{j}\alpha_{10}^{j}|R_m\right)=(2,3,4,3),\ r\left(\alpha_{5}^{j}\alpha_{11}^{j}|R_m\right)=(3,2,6,2),\\ r\left(\alpha_{5}^{j}\alpha_{12}^{j}|R_m\right)=(3,4,6,1),\ r\left(\alpha_{6}^{j}\alpha_{13}^{j}|R_m\right)=(4,5,7,0),\ r\left(\alpha_{7}^{j}\alpha_{14}^{j}|R_m\right)=(3,2,0,7),\\ r\left(\alpha_{8}^{j}\alpha_{15}^{j}|R_m\right)=(2,1,1,6),\ r\left(\alpha_{9}^{j}\alpha_{15}^{j}|R_m\right)=(2,2,2,5),\ r\left(\alpha_{10}^{j}\alpha_{16}^{j}|R_m\right)=(3,2,4,4),\\ r\left(\alpha_{10}^{j}\alpha_{17}^{j}|R_m\right)=(3,3,4,4),\ r\left(\alpha_{11}^{j}\alpha_{18}^{j}|R_m\right)=(4,3,5,2),\ r\left(\alpha_{12}^{j}\alpha_{18}^{j}|R_m\right)=(4,3,6,1),\\ r\left(\alpha_{13}^{j}\alpha_{19}^{j}|R_m\right)=(5,4,7,0).\end{aligned}$$

It is obvious by looking the position of every edge and every vertex, that there are no two edges having same code, there are no two vertices having the same code and there is no single edge having

the same code with any vertex. In short entire structure of perimantanes diamondoid with $\lambda = 1$, have unique representations. It is proved that the chosen subset is one of a possible candidate for the mixed metric resolving set with four minimum elements in it. □

Lemma 2.6. *Let PD_λ is a structure of perimantanes diamondoid with $\lambda = 1$. Then*

$$dim_m(PD_1) = 4. \tag{2.19}$$

Proof. The subset chosen in the Lemma 2.5 is a base case of this lemma. In the lemma, it is proved that $R_m = \{\beta_1, \beta_4, \alpha_7^1, \alpha_{13}^1\}$, is one of a candidate subset for the mixed-metric resolving set of structure of perimantanes diamondoid PD_1, and the structure shown in the Figure 1. Having four members in it, this proved that $dim_m(PD_1) \leq 4$. For the twofold inequality, chose contrary method and we will proved that $dim_m(PD_1) \neq 3$. Given below are some reasons on this assertion.

Let a chosen subset R'_m having three distinct elements, say $R'_m = \{\alpha_\xi^1, \alpha_1^j\}$, with distinct ξ, j. The contradiction will be arise due the either edges or edges which have two three and four distances to any of the chosen element of R'_m. Mathematically, it can be written as $r\left(\alpha_\alpha^1 | R'_m\right) = r\left(\alpha_\beta^1 | R'_m\right) = d\left(\alpha_\alpha^1, \alpha_\xi^1\right)$=(2, 3, 4) .

All the chosen cases resulted in the same location of at least two edges or two vertices. If both the edges and vertices have unique position, then the inter positions are matched for the structure and our main assertion resulted in the contradiction. So, it is proved that $dim_m(PD_1) \neq 3$.

Hence, $dim_m(PD_1) = 4$. □

Theorem 2.3. *Let PD_λ is a structure of perimantanes diamondoid with $\lambda \geq 2$. Then*

$$dim_m(PD_\lambda) = 2(\lambda + 1) \tag{2.20}$$

Proof. We will proved that the entire structure of perimantanes diamondoid have $dim_m(PD_\lambda)$=$2(\lambda + 1)$ for every possible value of $\lambda \geq 2$. For this prove, we will employ the technique of mathematical induction and the base case, which is for $\lambda = 1$ and $dim_m(PD_\lambda) = 4$, is already proved in the Lemmas 2.5 and 2.6.

Now, suppose the assertion is true for $\lambda = \chi$, and the equation becomes

$$dim_m\left(PD_\chi\right) = 2(\chi + 1). \tag{2.21}$$

We will show that it is true for $\lambda = \chi + 1$. Suppose

$$dim_m\left(PD_{\chi+1}\right) = dim_m\left(PD_\chi\right) + dim_m(PD_1) - 3. \tag{2.22}$$

Using Eqs 2.19 and 2.21 in Eq 2.22, we have

$$\begin{aligned} dim_m\left(PD_{\chi+1}\right) &= 2(\chi + 1) + 4 - 3, \\ &= 2(\chi + 1) + 1. \end{aligned} \tag{2.23}$$

As a result, the conclusion holds for all positive integers $\lambda \geq 1$.

Moreover, the generalized fault-tolerant edge resolving set for the generalized structure of perimantanes diamondoid, is in the set form is given by $R_m = \{\beta_1, \beta_{3\lambda+1}, \alpha_7^1, \alpha_7^2, \alpha_7^3, \ldots, \alpha_7^\lambda, \alpha_{13}^1, \alpha_{13}^2, \alpha_{13}^3, \ldots, \alpha_{13}^\lambda\}$. This concludes. □

3. Conclusions

In this article, we have discussed the edge metric dimension and their generalizations for the generalized perimantanes diamondoid structure and proved that each parameter depends on the copies of original or base perimantanes diamondoid structure and changes with the parameter n or its number of copies. Future direction can be considered as to discussed its other parameters which are also based on the metric of structure.

Conflict of interest

The authors declare no conflict of interest.

References

1. M. Diudea, C. Nagy, *Diamond and related nanostructures*, Netherlands: Springer, 2013. http://dx.doi.org/10.1007/978-94-007-6371-5
2. P. Schreiner, A. Fokin, H. Reisenauer, B. Tkachenko, E. Vass, M. Olmstead, et al., [123] tetramantane: parent of a new family of σ-helicenes, *J. Am. Chem. Soc.*, **131** (2009), 11292–11293. http://dx.doi.org/10.1021/ja904527g
3. M. Imran, M. Siddiqui, R. Naeem, On the metric dimension of generalized petersen multigraphs, *IEEE Access*, **6** (2018), 74328–74338. http://dx.doi.org/10.1109/access.2018.2883556
4. C. Wei, M. Nadeem, H. Siddiqui, M. Azeem, J. Liu, A. Khalil, On partition dimension of some cycle-related graphs, *Math. Probl. Eng.*, **2021** (2021), 4046909. http://dx.doi.org/10.1155/2021/4046909
5. M. Nadeem, M. Azeem, I. Farman, Comparative study of topological indices for capped and uncapped carbon nanotubes, *Polycycl. Aromat. Comp.*, in press. http://dx.doi.org/10.1080/10406638.2021.1903952
6. M. Nadeem, M. Azeem, H. Siddiqui, Comparative study of Zagreb indices for capped, semi-capped, and uncapped carbon nanotubes, *Polycycl. Aromat. Comp.*, in press. http://dx.doi.org/10.1080/10406638.2021.1890625
7. M. Nadeem, M. Imran, H. Siddiqui, M. Azeem, A. Khalil, Y. Ali, Topological aspects of metal-organic structure with the help of underlying networks, *Arab. J. Chem.*, **14** (2021), 103157. http://dx.doi.org/10.1016/j.arabjc.2021.103157
8. P. Slater, Leaves of trees, *Proceedings of the 6th Southeastern Conference on Combinatorics, Graph Theory, and Computing, Congressus Numerantium*, 1975, 549–559.
9. F. Harary, R. Melter, On the metric dimension of a graph, *Ars Combinatoria*, **2** (1976), 191–195.
10. G. Chartrand, E. Salehi, P. Zhang, The partition dimension of a graph, *Aequ. Math.*, **59** (2000), 45–54. http://dx.doi.org/10.1007/PL00000127
11. G. Chartrand, L. Eroh, M. Johnson, O. Oellermann, Resolvability in graphs and the metric dimension of a graph, *Discrete Appl. Math.*, **105** (2000), 99–113. http://dx.doi.org/10.1016/S0166-218X(00)00198-0

12. A. Kelenc, N. Tratnik, I. Yero, Uniquely identifying the edges of a graph: the edge metric dimension, *Discrete Appl. Math.*, **251** (2018), 204–220. http://dx.doi.org/10.1016/j.dam.2018.05.052

13. X. Liu, M. Ahsan, Z. Zahid, S. Ren, Fault-tolerant edge metric dimension of certain families of graphs, *AIMS Mathematics*, **6** (2021), 1140–1152. http://dx.doi.org/10.3934/math.2021069

14. A. Kelenc, D. Kuziak, A. Taranenko, I. Yero, Mixed metric dimension of graphs, *Appl. Math. Comput.*, **314** (2017), 429–438. http://dx.doi.org/10.1016/j.amc.2017.07.027

15. A. Ahmad, A. Koam, M. Siddiqui, M. Azeem, Resolvability of the starphene structure and applications in electronics, *Ain Shams Eng. J.*, **13** (2022), 101587. http://dx.doi.org/10.1016/j.asej.2021.09.014

16. A. Sebö, E. Tannier, On metric generators of graphs, *Math. Oper. Res.*, **29** (2004), 191–406. http://dx.doi.org/10.1287/moor.1030.0070

17. S. Khuller, B. Raghavachari, A. Rosenfeld, Landmarks in graphs, *Discrete Appl. Math.*, **70** (1996), 217–229. http://dx.doi.org/10.1016/0166-218X(95)00106-2

18. M. Johnson, Structure-activity maps for visualizing the graph variables arising in drug design, *J. Biopharm. Stat.*, **3** (1993), 203–236. http://dx.doi.org/10.1080/10543409308835060

19. M. Hauptmann, R. Schmied, C. Viehmann, Approximation complexity of metric dimension problem, *Journal of Discrete Algorithms*, **14** (2012), 214–222. http://dx.doi.org/10.1016/j.jda.2011.12.010

20. M. Garey, D. Johnson, *Computers and intractability: a guide to the theory of NP-completeness*, New York: W. H. Freeman & Co., 1990.

21. M. Johnson, Browsable structure-activity datasets, In: *Advances in molecular similarity*, London: JAI Press Connecticut, 1998, 153–170.

22. H. Raza, S. Hayat, X. Pan, On the fault-tolerant metric dimension of certain interconnection networks, *J. Appl. Math. Comput.*, **60** (2019), 517–535. http://dx.doi.org/10.1007/s12190-018-01225-y

23. Z. Ahmad, M. Chaudhary, A. Baig, M. Zahid, Fault-tolerant metric dimension of P(n, 2)⊙K1 graph, *J. Discrete Math. Sci. C.*, **24** (2021), 647–656. http://dx.doi.org/10.1080/09720529.2021.1899209

24. J. Liu, Y. Bao, W. Zheng, S. Hayat, Network coherence analysis on a family of nested weighted n-polygon networks, *Fractals*, **29** (2021), 215260. http://dx.doi.org/10.1142/s0218348x21502601

25. M. Javaid, M. Aslam, J. Liu, On the upper bounds of fractional metric dimension of symmetric networks, *J. Math.*, **2021** (2021), 8417127. http://dx.doi.org/10.1155/2021/8417127

26. D. Vietz, E. Wanke, The fault-tolerant metric dimension of cographs, In: *Fundamentals of computation theory*, Cham: Springer, 2019, 350–364. http://dx.doi.org/10.1007/978-3-030-25027-0_24

27. S. Sharma, V. Bhat, Fault-tolerant metric dimension of two-fold heptagonal-nonagonal circular ladder, *Discret. Math. Algorit.*, **14** (2022), 2150132. http://dx.doi.org/10.1142/s1793830921501329

28. L. Saha, Fault-tolerant metric dimension of cube of paths, *J. Phys.: Conf. Ser.*, **1714** (2021), 012029. http://dx.doi.org/10.1088/1742-6596/1714/1/012029

29. Y. Huang, B. Hou, W. Liu, L. Wu, S. Rainwater, S. Gao, On approximation algorithm for the edge metric dimension problem, *Theor. Comput. Sci.*, **853** (2021) 2–6. http://dx.doi.org/10.1016/j.tcs.2020.05.005
30. M. Ahsan, Z. Zahid, S. Zafar, A. Rafiq, M. Sindhu, M. Umar, Computing the edge metric dimension of convex polytopes related graphs, *J. Math. Comput. Sci.-JM*, **22** (2020), 174–188. http://dx.doi.org/10.22436/jmcs.022.02.08
31. A. Koam, A. Ahmad, Barycentric subdivision of Cayley graphs with constant edge metric dimension, *IEEE Access*, **8** (2020), 80624–80628. http://dx.doi.org/10.1109/ACCESS.2020.2990109
32. Z. Raza, M. Bataineh, The comparative analysis of metric edge metric dimension of some subdivisions of the wheel graph, *Asian-Eur. J. Math.*, **14** (2021), 2150062. http://dx.doi.org/10.1142/S1793557121500625
33. J. Liu, Z. Zahid, R. Nasir, W. Nazeer, Edge version of metric dimension anddoubly resolving sets of the necklace graph, *Mathematics*, **6** (2018), 243. http://dx.doi.org/10.3390/math6110243
34. T. Iqbal, M. Azhar, S. Bokhary, The k-size edge metric dimension of graphs, *J. Math.*, **2020** (2020), 1023175. http://dx.doi.org/10.1155/2020/1023175
35. M. Wei, J. Yue, X. Zhu, On the edge metric dimension of graphs, *AIMS Mathematics*, **5** (2020), 4459–4465. http://dx.doi.org/10.3934/math.2020286
36. B. Deng. M. Nadeem, M. Azeem, On the edge metric dimension of different families of Möbius networks, *Math. Probl. Eng.*, **2021** (2021), 6623208. http://dx.doi.org/10.1155/2021/6623208
37. A. Koam, A. Ahmad, M. Ibrahim, M. Azeem, Edge metric fault-tolerant edge metric dimension of hollow coronoid, *Mathematics*, **9** (2021), 1405. http://dx.doi.org/10.3390/math9121405
38. M. Bataineh, N. Siddiqui, Z. Raza, Edge metric dimension of k-multiwheel graph, *Rocky Mountain J. Math.*, **50** (2020), 1175–1180. http://dx.doi.org/10.1216/rmj.2020.50.1175
39. H. Raza, Y. Ji, Computing the mixed metric dimension of a generalized petersengraph $P(n, 2)$, *Front. Phys.*, **8** (2020), 211. http://dx.doi.org/10.3389/fphy.2020.00211
40. H. Raza, J. Liu, S. Qu, On mixed metric dimension of rotationally symmetric graphs, *IEEE Access*, **8** (2019), 11560–11569. http://dx.doi.org/10.1109/ACCESS.2019.2961191
41. H. Raza, Y. Ji, S. Qu, On mixed metric dimension of some path related graphs, *IEEE Access*, **8** (2020), 188146–188153. http://dx.doi.org/10.1109/ACCESS.2020.3030713
42. M. Azeem, M. Nadeem, Metric-based resolvability of polycyclic aromatic hydrocarbons, *Eur. Phys. J. Plus*, **136** (2021), 395. http://dx.doi.org/10.1140/epjp/s13360-021-01399-8
43. A. Ahmad, S. Husain, M. Azeem, K. Elahi, M. Siddiqui, Computation of edge resolvability of benzenoid tripod structure, *J. Math.*, **2021** (2021), 9336540. http://dx.doi.org/10.1155/2021/9336540
44. M. Imran, A. Ahmad, M. Azeem, K. Elahi, Metric-based resolvability of quartz structure, *Comput. Mater. Con.*, **71** (2022), 2053–2071. http://dx.doi.org/10.32604/cmc.2022.022064
45. H. Siddiqui, M. Imran, Computing the metric and partition dimension of H-Naphtalenic and VC5C7 nanotubes, *J. Optoelectron. Adv. M.*, **17** (2015), 790–794.

46. H. Siddiqui, M. Imran, Computing metric and partition dimension of 2-dimensional lattices of certain nanotubes, *J. Comput. Theor. Nanos.*, **11** (2014), 2419–2423.